fire

MDPI

Article

A Real-Time Pre-Response Experiment System for High-Rise Building Fires Based on the Internet of Things

Haoyou Zhao, Zhaoyang Yu * and Jinpeng Zhu

Mining College, Guizhou University, Guiyang 550025, China; zhaohaoyou233@163.com (H.Z.); dagwbl@outlook.com (J.Z.)
* Correspondence: zyyu@gzu.edu.cn

Abstract: The primary objective of the current fire protection system in high-rise buildings is to extinguish fires in close proximity to the detectors. However, in the event of rapidly spreading fires, it is more effective to limit the transmission of fire and smoke. This study aims to develop an IoT-based real-time pre-response system for high-rise building fires that is capable of limiting the spread of fire and smoke. The proposed system collects fire data from sensors and transmits them to a cloud computer for real-time analysis. Based on the analysis results, the cloud computer controls the actions of alarm devices, ventilation equipment, and fine water mist nozzles. The system can dynamically adjust the entire system's behavior in real time by adopting pre-response measures to extinguish fires and limit the spread of fires and smoke. The system was tested on a simulation platform similar to actual high-rise buildings to evaluate its impact on fires and smoke. The results demonstrate the system's effectiveness in extinguishing fires and suppressing the spread of fires and smoke.

Keywords: high-rise building; fire; smoke; Internet of Thing

Citation: Zhao, H.; Yu, Z.; Zhu, J. A Real-Time Pre-Response Experiment System for High-Rise Building Fires Based on the Internet of Things. *Fire* **2023**, *6*, 271. https://doi.org/10.3390/fire6070271

Academic Editor: Tiago Miguel Ferreira

Received: 29 May 2023
Revised: 25 June 2023
Accepted: 6 July 2023
Published: 9 July 2023

1. Introduction

Natural and man-made disasters pose significant threats to the environment and human life worldwide. Among these disasters, fires are one of the most destructive threats, causing the highest number of human casualties [1]. High-rise building fires, in particular, cause severe damage due to their complex functions, numerous occupants, vast internal areas, and significant amounts of electrical and heating equipment. This makes them highly susceptible to fires [2]. Once a high-rise building catches fire, evacuation becomes a significant challenge due to the large number of occupants and the vast area [3]. Power outages caused by high-rise building fires can make it difficult to assess the extent of the fire and hinder firefighting efforts [4]. Additionally, the height of high-rise buildings increases the difficulty of external rescue and firefighting [5]. Therefore, the development of high-rise building fire protection systems is crucial.

Traditional fire protection systems have many limitations [6,7]. Most high-rise building fires start as small local fires, gradually spreading to other locations and developing into large fires [8,9]. Thus, high-rise building fire protection systems need to detect and extinguish fires promptly, preventing small fires from escalating into large ones. Even if the fire cannot be controlled, it is crucial to limit the fire and smoke to a certain area, providing time for evacuation and firefighting. Traditional high-rise building fire protection systems typically initiate water spray and alarm when the temperature reaches a certain threshold [10]. These continuously spray water until it is depleted or security personnel manually turn off the alarm. This method lacks the ability to autonomously identify the size of the fire and whether the fire is extinguished [11]. Fire curtains and positive pressure ventilation devices used to create fire protection zones and limit the spread of fire and smoke can only be manually controlled near the devices. This can hinder evacuations and external rescue [12]. Traditional high-rise building fire sprinkler systems cannot be stopped until manually turned off [13]. Adding a signal judgment device between the sprinkler

device and detector is one way to solve the problem, but this can result in significant cost increases [14]. In addition, the reliability of a single signal judgment device is low [15]. The continuous spraying of water can cause damage to appliances and instruments in the room, which may result in greater losses than from the fire [16]. Even if the fire appears to be extinguished on the surface, there is still a risk of re-ignition [17]. Open-type sprinklers are designed for one-time use and cannot be restarted. Traditional fire protection systems are powerless against re-igniting fires [18]. The repeated opening and closing pre-action system can spray water to extinguish fires after re-ignition and automatically shut down the system after the fire is extinguished [19]. However, this system is expensive and requires a long and complex circuit design, and its reliability is questionable in practical use. Investigating fires after they occur requires fire scene data [20]. Most traditional fire protection systems do not have data-recording capabilities. Some fire control systems can store detector data and record the entire system's operation, but the data are stored on the host in the fire control room [21]. This method is not safe in the face of devastating fires [18]. Traditional high-rise building fire protection systems can no longer meet the increasingly complex needs of high-rise buildings for fire protection systems. Actively introducing new methods, such as big data and computer-assisted decision-making, to study new information-based and intelligent high-rise building fire protection systems is of great significance [22].

The Internet of Things (IoT) is one of the most promising application prospects for new methods. IoT combines various information sensing devices, controllers, and action devices through a network to form a huge network, thereby achieving the technical ability to control all devices anytime and anywhere [23]. This study designed a system that relies on IoT technology and wireless transmission technologies, such as Wi-Fi, to transmit fire data collected by sensors to cloud computers in real-time. The cloud computer analyzes the data in real-time through pre-set programs, thereby controlling the action of alarm devices, ventilation devices, water spray nozzles, and other action devices. In this study, the system was installed on a small and similar platform to verify its capabilities.

2. Establishment of a Real-Time Pre-Response System

This section proposes a real-time dynamic pre-response system based on the Internet of Things (IoT) for high-rise buildings. The system's primary objective is to quickly extinguish fires while confining them to a specific area. The system recognizes fire signals as normal, warning, general fire, and major fire states, and responds accordingly with no response, the alarm, the first-level response, or the second-level response. By leveraging IoT technology and wireless transmission, the system collects fire data from sensors and transmits them to cloud computers for real-time analysis. The analysis results are then used by the cloud computer to control the actions of alarm devices, ventilation devices, and water spray nozzles. Compared to traditional high-rise building fire protection systems, the proposed system can dynamically adjust its behavior in real time and take preemptive action to extinguish fires and limit their spread. Furthermore, the system's powerful computing capability facilitates reliable analysis and signal processing through cloud computers. The use of wireless transmission devices enhances the system's reliability.

2.1. A Prediction Model for Smoke Spread Path

To confine fires and smoke to a specific area, understanding the priority of the spread paths is crucial. This study employs graph theory, a branch of discrete mathematics that uses graphs as a research object [24], to investigate the spread paths of high-rise building fires. The core concepts of graph theory are vertices and edges, where the vertices represent the research entities, such as locations or people, and the edges represent specific relationships between two vertices. In this model, independent spaces, such as rooms, corridors, and staircases, are treated as vertices, while channels that allow for the direct transmission of smoke between two independent spaces are treated as edges.

Abstract Building as DAG Network Model

Directed acyclic graphs (DAGs) are widely used data structures in computer science. Their unique topological structure allows them to exhibit excellent properties in various algorithmic scenarios, such as dynamic programming, shortest path search in navigation, and data compression [25]. In high-rise buildings, rooms, corridors, and vertical passages where fires may occur are represented as nodes, while the possible propagation directions between nodes are represented as edges. A network model schematic of the high-rise building was created and is shown in Figure 1. In the figure, the gray area represents nodes and the black area represents edges.

Figure 1. Schematic diagram of abstracting high-rise buildings into network models.

Abstracting a high-rise building as a directed acyclic graph (DAG) involves six steps. First, each room or area in the building is identified and allocated a unique identifier or node name. Second, the relationships among the rooms or areas are determined. This includes the doors or passages between rooms, and passages such as stairs or elevators are determined and represented as directed edges, with arrows pointing from one room or area to another. Third, the dependencies among the rooms or areas are determined. This includes some rooms or areas that can only be accessed through others or must be accessed after the completion of other rooms or areas, and are represented as directed edges. Fourth, the graph is checked for cycles and decomposed into smaller components until each component is a DAG if cycles are present. Fifth, weights are assigned to each node in the graph based on the area or usage of each room and its fire load. Finally, the graph is visualized to facilitate better understanding and analysis.

Channels in a high-rise building can be abstracted as single or multiple nodes. Generally, connected horizontal and vertical passageways, such as corridors and elevators, are abstracted as a single node [26]. However, during a fire, these passageways are not homogeneous, and the distribution of physical parameters, such as the smoke density and temperature, is not consistent [27]. A single node cannot accurately describe this non-homogeneous physical state, potentially leading to confusing and inaccurate simulation results based on graph theory. To overcome this limitation, this study proposes a detailed abstraction of horizontal and vertical passageways, dividing them into multiple nodes based on the geometric dimensions of rooms and floors, as shown in Figure 2. These nodes generally have different physical state attribute values in the actual physical process. White nodes represent rooms, gray nodes represent corridors, red nodes represent the room on fire, green nodes represent staircases, and blue nodes represent the atmosphere. Additionally, to facilitate algorithm processing, conventional room numbers need to be flattened using the flattening algorithm shown in Equation (1).

$$ID_f = (F - 1) \times 10 + R \quad (1)$$

where ID_f is the flattened unique ID, F represents the floor number, and R represents the Rth room on the F floor. The floor numbering is illustrated in Figure 2.

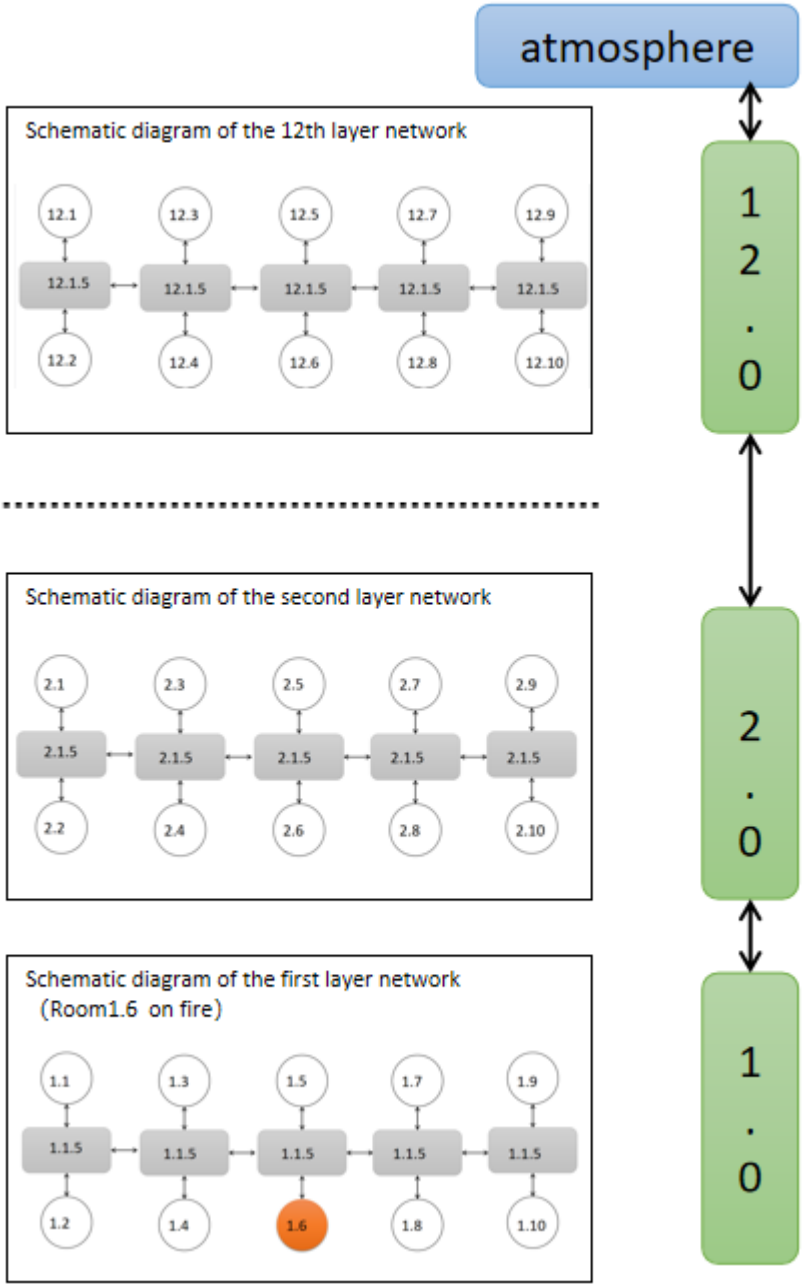

Figure 2. Long channel abstracted as a multi-node schematic diagram.

High-rise building fires involve complex physical scenarios that require assumptions and simplifications. These include smoke production mechanisms from burning fuel, mixed flow of smoke and air, heat and thermal radiation exchange with the building materials, and a series of physical processes [28,29]. To identify the factors that play a determining role, studies of these processes require making certain assumptions and simplifications.

(1) Ignoring smoke spreading to the outside through holes such as windows, the model focuses on the transfer of smoke from rooms to horizontal and vertical passages. Therefore, only adjacent corridor nodes have edges with each room.

(2) The ratio of smoke production to heat release is simplified to 1:1 per unit of time. Although smoke production varies for different materials, it is always proportional to the

heat release rate during combustion. Therefore, it is assumed that there is a 1:1 proportion between smoke production and heat release.

(3) It is assumed that smoke spread follows the permeation law. That is, the smoke capacity of each node is limited, and smoke is easily compressed. Smoke will spread from areas of high concentration to areas of low concentration, high temperature to low temperature, and high pressure to low pressure. Although smoke spreading involves multiple physical fields and is influenced by factors such as temperature, pressure, and wind speed, the study assumes each node has a certain smoke capacity [30]. When the smoke is saturated, only the temperature will increase, and no change in smoke concentration will occur.

(4) It is assumed that the smoke capacity of the atmospheric environment nodes is infinite.

In the simulation program, the ignition point starts the fire. The simulation ends when the ignition point stops releasing heat, and the smoke no longer flows violently. The heat release process is shown in Figure 3.

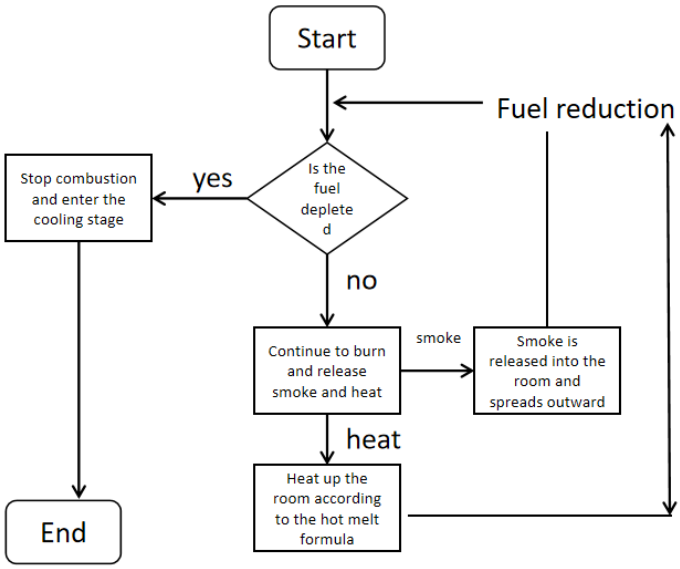

Figure 3. Schematic diagram of heat release process.

The weights assigned to each edge in the network model depend on the relationships among the nodes. Each edge is assigned a weight representing the volume of smoke flowing from tail to head per unit of time. Since smoke overflow to the external atmosphere is ignored, all nodes satisfy Kirchhoff's law. The inflow of smoke at each node equals the outflow, as shown in Equation (2) [31]. The size of each room corresponds to the smoke saturation level at the corresponding node.

$$\sum_{k=1}^{n} i_k = 0, \tag{2}$$

where i_k represents the smoke flow at the ith node. If the node has not reached the saturation state, the weight of the smoke stored in the node can be expressed as Equation (3).

$$w_t = 1 - \frac{C_t}{C_a}, \tag{3}$$

where C_t represents the current smoke volume, C_a represents the smoke capacity of the node, and w_t denotes the weight of the smoke when the node has not reached saturation.

The Networkx and Matplotlib packages can be used to easily implement the overall framework and responsive logic of the code, as demonstrated in the visualization example

in Figure 4 [32]. The figure illustrates the different nodes used in the simulation. The red node represents the ignition point, the dark red nodes represent horizontal passageways mainly used as corridors, the blue node represents the atmospheric environment, the green nodes represent vertical passageways, and the yellow nodes represent conventional rooms. However, in actual high-rise buildings, the large number of nodes may make it difficult to discern the visualization results. For display convenience, the building in the example was limited to five floors, with only six rooms per floor. The simulation began with rooms (1, 4) as the ignition point, and the results are presented in Figure 5. In Figure 5, the red node represents the room on fire, the yellow node represents the room, the brown node represents the corridor, the green node represents the staircase, and the blue node represents the external atmosphere.

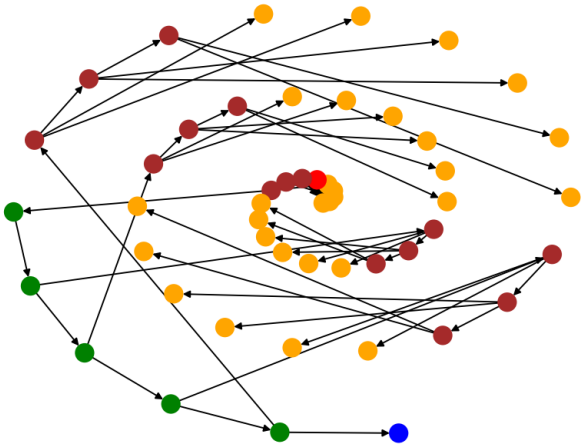

Figure 4. Visualization of high-rise buildings in graph theory model.

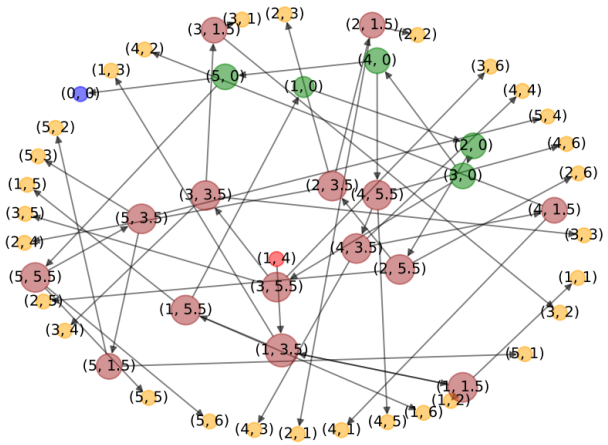

Figure 5. Architectural visualization of 6 rooms on each floor of a 5-story building.

Table 1 shows the smoke situation of each node after the simulation. Since the smoke content of each node did not reach its maximum during the simulation, the speed at which smoke entered each node was roughly the same. Therefore, the smoke content of each node in Table 1 can be considered an indicator of the smoke flow rate, with higher smoke content indicating a faster smoke flow rate at the node. This means that smoke was more likely to reach that node first, reflecting the degree of susceptibility to smoke propagation among the nodes. In the table, it can be seen that the smoke content of the ignition floor was ranked in descending order as (1, 4), (1, 3.5), (1, 3), (1, 1.5), (1, 5.5), (1, 1), (1, 2), (1, 5), (1, 6), and (1, 0). In summary, the ignition room had the highest smoke content, followed by the adjacent corridor, adjacent rooms and corridors, other rooms, and finally, the staircase.

Table 1. Computer simulation results of node smoke content.

Node	Smoke Content	Node	Smoke Content
(1, 1)	116,443.78	(3, 5.5)	2918.91
(1, 2)	116,443.78	(4, 1)	27.12
(1, 3)	299,361.92	(4, 2)	27.12
(1, 4)	1,196,204.44	(4, 3)	48.37
(1, 5)	116,443.78	(4, 4)	48.37
(1, 6)	116,443.78	(4, 5)	159.35
(1, 1.5)	299,361.92	(4, 6)	159.35
(1, 3.5)	652,390.65	(4, 1.5)	48.37
(1, 5.5)	299,361.92	(4, 3.5)	159.35
(2, 1)	159.35	(4, 5.5)	685.19
(2, 2)	159.35	(5, 1)	23.36
(2, 3)	685.19	(5, 2)	23.36
(2, 4)	685.19	(5, 3)	27.12
(2, 5)	2918.91	(5, 4)	27.12
(2, 6)	2918.91	(5, 5)	48.37
(2, 1.5)	685.19	(5, 6)	48.37
(2, 3.5)	2918.91	(5, 1.5)	27.12
(2, 5.5)	11,320.71	(5, 3.5)	48.37
(3, 1)	48.37	(5, 5.5)	159.35
(3, 2)	48.37	(1, 0)	116,443.78
(3, 3)	159.35	(2, 0)	38,893.92
(3, 4)	159.35	(3, 0)	11,320.71
(3, 5)	685.19	(4, 0)	2918.91
(3, 6)	685.19	(5, 0)	685.19
(3, 1.5)	159.35	(0, 0)	159.35
(3, 3.5)	685.19		

The smoke content of the second and ignition floors differed. On the second floor, the smoke content was ranked in descending order as (2, 0), (2, 5.5), (2, 3.5), (2, 5), (2, 6), (2, 1.5), (2, 4), (2, 3), (2, 2), and (2, 1). Based on the analysis, the smoke content was ranked in descending order as highest in the staircase, followed by the room near the staircase in the corridor, the rooms in the middle and near the staircase in the corridor, the middle rooms far from the staircase, and finally, the rooms far from the staircase. The smoke distribution on other floors was similar, with the smoke content ranked in descending order as highest in the staircase, followed by the room near the staircase in the corridor, the rooms in the middle and near the staircase in the corridor, the middle rooms far from the staircase, and finally, the rooms far from the staircase.

The study revealed that the smoke content of different nodes can help infer the path of smoke propagation. On the ignition floor, smoke entered the corridor from the ignition room and then spread to other rooms and vertical passageways from the corridor. Smoke was mainly discharged outdoors or spread to other floors via the vertical passageway. On non-ignition floors, smoke entered the corridor from the vertical passageway and then spread to different rooms based on their proximity to the vertical passageway. By analyzing the extent of spread from the ignition room, the nodes that were most susceptible to fire spread during high-rise building fires could be identified. These nodes should be given priority when considering pre-response control strategies.

2.2. Real-Time Dynamic Pre-Response Strategies

The pre-response strategy's fundamental logic comprises three parts: Query, Calculate, and Action, as illustrated in Figure 6. The system operates in a 24 h cycle, continuously monitoring the environmental temperature. When the temperature surpasses a particular threshold, the system initiates a series of actions to respond to high temperatures or fire situations. The Query component sends the raw data to the Calculate component for computation when the temperature surpasses the threshold, and the calculation results are

then sent to the Action component. The Action component executes various operations, such as activating the spray system, and then sends the results back to the Query component for verification.

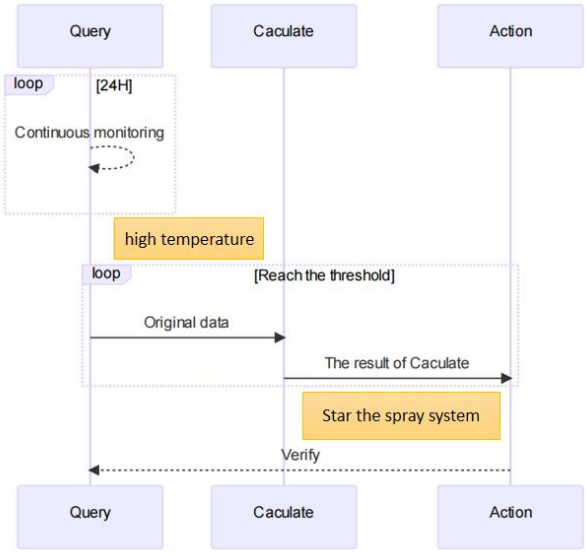

Figure 6. System pre-response logic.

2.2.1. Pre-Response Action Logic

The pre-response logic needs to be set in advance in the program. According to the analysis of fire and smoke propagation paths in high-rise buildings and computer simulation studies, fire and smoke spreading to adjacent areas have priority. Based on the priority of each room's spread, the order of priority is as follows: rooms on the upper adjacent floors, rooms on the left and right adjacent floors, corridors and rooms on the opposite side, horizontal passageways, and vertical passageways. To achieve a pre-response before a fire occurs, the relationship between the spread priority of each room must be represented in the computer. The server evaluates the signals received by the detector at regular intervals. Temperature signals are classified as a warning status, first-level response, or second-level response, based on the temperature from low to high, respectively. The temperature settings are determined based on the building type and detector location, defaulting to 57 °C, 77 °C, and 120 °C. Gas detector signals are similarly classified into three levels of response when an initial fire occurs but the temperature or gas concentration has not yet reached the threshold for activating the high-rise building fire real-time pre-response system. This is the warning stage, and alarms and warnings should be issued to alert people. After confirming that there is no fire, the alarm can be manually or remotely turned off. From the warning stage, the interval for evaluating the signals collected by the detectors in this area is reduced by half. When the temperature or gas concentration reaches the first-level response temperature, the first-level pre-response is activated for control, and the potential second-level pre-response endpoint enters the warning status. In addition to initiating the alarm, the fine water mist nozzles in the response room are activated to attempt to extinguish the fire as soon as possible. When the fire continues to spread and the ignition room undergoes a flashover, the second-level pre-response is activated. Based on the path prediction of fire and smoke propagation studied using graph theory in the previous section, the priority of fire and smoke spreading to other areas is determined. The fine water mist nozzles in the rooms, corridors, and stairwells with high priority are activated to block the spread of smoke and flames. When the system initiates a response, the signals from the detectors at the same location are subjected to OR logic. That is, if any signal indicates a particular response level, the response is initiated, and the system responds according to the highest signal level received. The response level of the detectors in the area that have already responded decreases as the information about the

temperature or gas concentration collected by the detectors in that area decreases, until the response is stopped. If the signals from more than half of the detectors in the same fire compartment indicate the same response level, the system responds at a higher level.

2.2.2. Response Strategy Reliability Verification

This study utilized computer simulations to verify the reliability of the system, and the entire simulation experiment process was implemented using object-oriented programming in Python. The Room class and Building class were created based on this method. The Room class represents a basic unit of a room, including the indoor temperature, location, nozzle switch status, and nozzle switch temperature threshold. These are represented by the temperature, location, sprinkle, and threshold, respectively. The Building class represents a complete building, including the environmental temperature, number of floors, number of rooms per floor, and the properties of the first-level and second-level pre-response control. The entire digital building was constructed by using the generate_rooms() method to instantiate several Room class objects and then storing their instances in a Building class. The program structure of the Building class is shown in Figure 7. In addition to the verification system, the Building class also implements multiple functions, such as adjudge_location(), get_control_vex(), convert_room_id(), pre_control(), and ignite(). These are used for fire location determination, control vector acquisition, flattening room IDs, pre-control, and simulating random ignition, respectively.

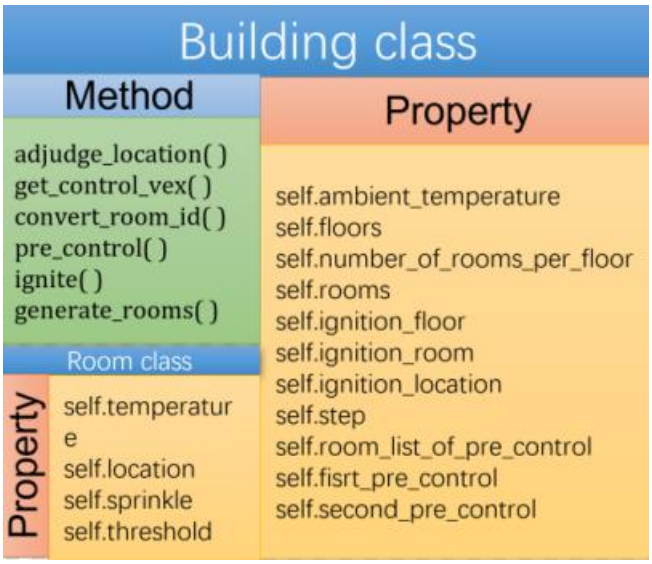

Figure 7. Building class structure in simulation programs.

In this study, the heating formula was incorporated into the Building class, and random terms were included to simulate random effects during actual heating. The simulation experiment was conducted using the Random module to randomly select building and room numbers to ignite corresponding rooms. The time of the pre-response level occurrence, the room temperature at the response time, and the corresponding pre-response vector were recorded. The experimental results are summarized in Table 2. Equation (4) was used in this study.

$$\frac{T_g - T_0}{T_{gm} - T_0} = \left[\frac{t}{t_m}.\exp(1 - \frac{t}{t_m})\right]^{0.8} \quad (4)$$

where t is the fire duration (min); T_g is the average temperature of the hot smoke gas at time t (°C); T_{gm} is the maximum temperature that the hot smoke gas layer can reach (°C); t_m is the average time to reach the maximum temperature (min); T_0 is the indoor temperature before the fire occurs (°C).

Table 2. Reliability results.

Response Level	Expected Response Time (s)	Average Response Time (s)	Setting Temperature (°C)	Average Response Temperature (°C)
Level 1	16.2	31.3	70	86
Level 2	439	506	600	618

To verify the reliability of the response, the response delay time was observed. The first-level pre-response temperature was set to 70 °C, and the second-level pre-response temperature was set to 600 °C. It was observed that during the first-level response, the average response time was delayed by 15.1 s, with an average response error temperature of 26 °C. During the second-level response, the average response time was delayed by 67 s, with an average response error temperature of 18 °C. Under the conditions of temperature changes with added random values, the average response time error of the system was less than 20 s, and the average response temperature error was less than 20 °C. These results indicate that the system met the response requirements.

2.3. System Framework and Architecture

2.3.1. System Components

ESP8266 module;
Relay module;
DHT11 temperature and humidity sensor;
MQ-135 gas sensor;
Optocoupler isolation switch;
Signal indicator light;
K-type thermocouple;
Max6675 module;
Water mist nozzle;
PMS7003T.

2.3.2. System Functional Framework

The system presented in this paper comprises four parts: the perception and control layer, the network layer, the service layer, and the application layer. Each layer has corresponding functional modules. The overall architecture is depicted in Figure 8. The perception and control layer consists of two parts: perception and control. The perception segment includes a K-type thermocouple, an MQ-135 gas sensor, and a DHT11 temperature and humidity sensor, which detect and transmit environmental data to the microcontroller unit (MCU). The control portion is mainly composed of relays, which regulate the fine water mist nozzles, alarms, fans, lighting facilities, and other equipment. The network layer provides internal communication channels for the system, transmitting information from the perception and control layer to the service layer. The network layer consists of routers, external API interfaces, and wired networks. The service layer serves as the control and computing center of the entire system, comprising cloud servers, databases, storage hard disks, and switches. The service layer analyzes and evaluates the obtained data, actively issuing control instructions based on the built-in algorithm, and receiving instructions from the application layer. The application layer provides an API interaction interface between humans and the system, enabling users to query information from the service layer and issue control instructions. The application layer includes display devices, data-processing systems, and system operation devices.

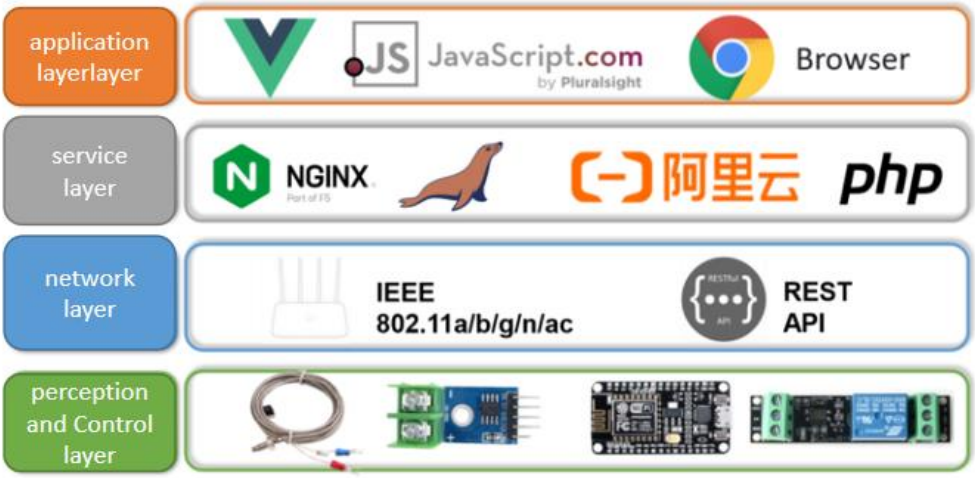

Figure 8. Overall system structure.

2.3.3. System Topology

This paper presents a system composed of multiple components, including sensors, data processors, and actuators. The system topology diagram is depicted in Figure 9. The sensors can collect various data, such as the temperature, smoke, and carbon monoxide levels. The data processor is located on the server and is responsible for identifying, analyzing, and making decisions based on the data collected by the sensors. The actuators, such as optocoupler isolation switches, relays, nozzles, and alarms, execute the tasks issued by the data processor.

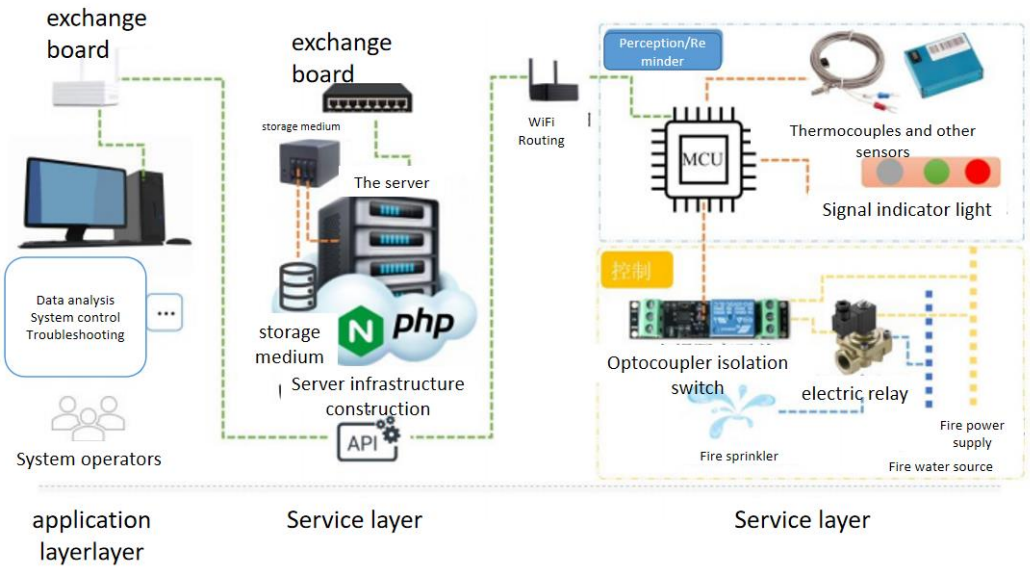

Figure 9. System topology diagram.

2.3.4. System Workflow Description

The system workflow comprises six steps. The first step is sensor data acquisition. Multiple sensors, including gas and temperature sensors, collect real-time environmental data. The gas sensor used in this system was the MQ-135 gas sensor, which uses SnO_2 as the gas-sensitive material. When the sensor is exposed to polluted air, its conductivity increases with the concentration of the pollutant. Multiple MQ135 gas sensors were set to different working modes to collect data on different gases. The temperature sensor was a K-type thermocouple, which was used with MAX6675 to convert the temperature signal into a digital signal for subsequent analysis. The next step is data transmission. The data collected by the sensors are uploaded to a cloud server for processing through the Internet

of Things (IoT) technology. Then, the data-processing and intelligent decision-making stage follows. The cloud server analyzes the data based on the set intelligent algorithm and makes intelligent decisions, such as determining which areas need to activate the automatic sprinkler system and adjusting the range and intensity of the sprinkler. The intelligent algorithm and decision-making are established based on the response strategy given in Section 2.2. The final steps are control execution and message alarm. These two steps are carried out simultaneously. The system controls the automatic sprinkler system to start using the actuators to effectively extinguish fires in the target area. It also provides real-time message alerts and alarm functions, promptly notifying relevant personnel, such as administrators and owners, to quickly respond to dangerous situations, such as fire.

2.3.5. Software Architecture (System Source Code Development)

The system and software described in this paper were developed using the Python programming language and the Thonny integrated development environment. Figure 10 displays a flowchart of the system's source code.

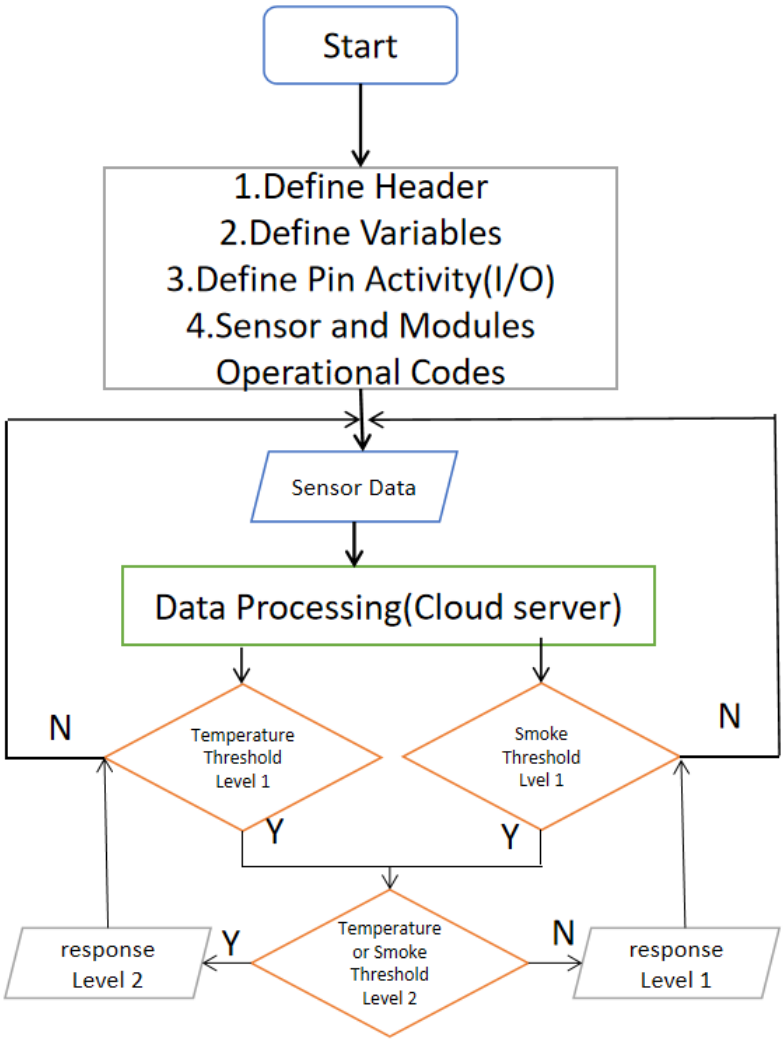

Figure 10. System source code flowchart.

3. Evaluation of the System

The aim of this section is to assess the responsiveness and fire suppression effectiveness of the system. Small-scale experiments were conducted on a high-rise building fire simulation platform based on similarity criteria. Multiple experiments were performed to analyze the system's response to fires under different conditions, and some of them were

selected to verify the system's effectiveness. During the experiment, real-time temperature monitoring data were recorded, and different response strategies were applied. Initially, we created a similarity model of a high-rise building to simulate the temperature and smoke changes in a real fire environment. Subsequently, we used IoT technology to connect sensors, controllers, and sprinklers, enabling a high-precision and fast-response automatic sprinkler system. During the experiment, water was sprayed based on the set sprinkler time and water quantity in response to changes in the fire temperature and smoke. Finally, we collected the fire temperature data and smoke conditions under various parameters.

3.1. Methods

For this experiment, an ideal high-rise building model was constructed. The building had nine stories, and each floor was 3 m tall, resulting in a total height of 27 m. Each floor contained ten rooms, a stairwell, an elevator shaft, and a stair landing. Figure 11 displays a top-view schematic of the model. The experiment was carried out on a small-scale similarity simulation platform for high-rise building fires. The experimental platform was primarily made of stainless steel, as shown in Figure 12, and followed the Froude similarity criterion with a scale ratio of 1/10. Table 3 summarizes the relationships between some of the physical parameters of the model and the prototype. The prototype fire load density for hotels and offices, 480 MJ/m^2, was used as the mean fire load density. Two different sizes of combustion boxes (10 cm × 10 cm and 15 cm × 15 cm) were used to measure two different fire source powers (heat release rates) using the mass loss method. The measured heat release rates were 2.4 kW and 5.7 kW, respectively [33,34]. The system was installed on the experimental platform. As shown in Figure 12, the system was installed on the first three layers of the experimental platform. The role of the system was analyzed by recording its impact on the temperature and smoke conditions under different fire conditions. The system response time was recorded to analyze the timeliness of the system response. Multiple sets of experiments were conducted, and the adjusted parameters included the position of the fire source, the heat release rate, and whether to activate the system's response function.

Table 3. Froud's similarity criterion relationship.

Physical Parameters	Proportional Relationship	Formula Number
Heat release rate (Kw)	$Q_P = Q_M(L_P/L_M)^{5/2}$	Equation (5a)
Volume flow rate (m^3/s)	$V_P = V_M(L_P/L_M)^{5/2}$	Equation (5b)
Time (s)	$t_P = t_M(L_P/L_M)^{1/2}$	Equation (5c)
Speed (m/s)	$v_P = v_M(L_P/L_M)^{1/2}$	Equation (5d)
Quality (Kg)	$m_P = m_M(L_P/L_M)^3$	Equation (5e)
Temperature (K)	$T_P = T_M$	Equation (5f)
Fire load (MJ)	$q_p = q_m(L_P/L_M)^4$	Equation (5g)

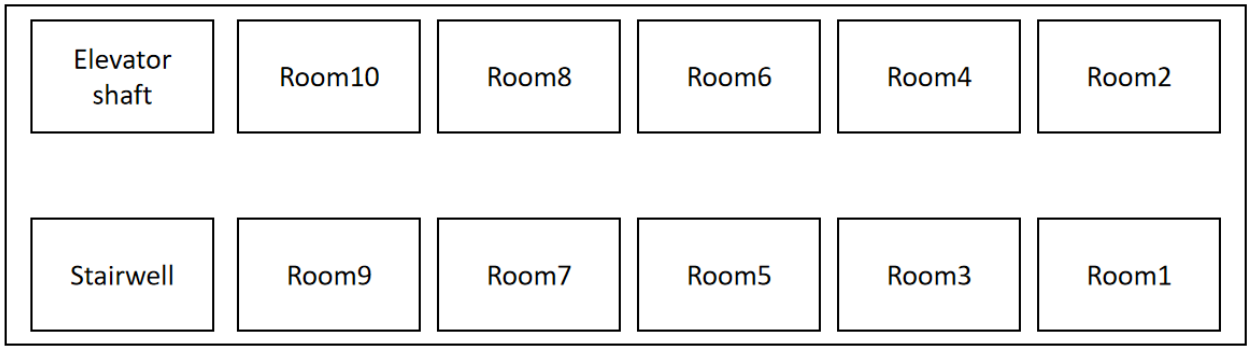

Figure 11. Top-view schematic diagram of the model.

Figure 12. Model appearance.

3.2. Results

The authors of this paper selected four experimental groups to visualize the distribution of the node temperatures. The specific experimental conditions are detailed in Table 4. Experiments 8-12 and 8-13 were conducted under an ambient temperature of 0 °C. Experiments 10-1 and 10-2 were conducted under an ambient temperature of 23 °C.

Table 4. Similar simulated experimental conditions for experiments 8-13, 8-12, 10-1, and 10-2.

Experiment Number	Fire Location	Heat Release Rate (kw)	System Response Status
8-13	(2.9)	5.7	No
8-12	(2.9)	5.7	Yes
10-1	(10.9)	2.4	No
10-2	(10.9)	2.4	Yes

3.2.1. The Impact of the System on the Temperature of High-Rise Building Fires

This study analyzed temperature changes to investigate the ability of this system to extinguish fires and limit fire spread. First, the case of a high heat release rate was considered. Figures 13 and 14 plot the temperature information of the fire room and corridor under four different experimental conditions. The orange curve represents the temperature without the system, while the blue curve represents the temperature with the system activated. In Figure 13, 2-9 represents the fire room located on the second floor with room number 9. Before the system was applied, the temperature in this room reached a maximum of 200 °C, but after the system was applied, the maximum temperature was only 130 °C. In Figure 13, 2-7.5 represents the corridor between rooms 2-7 and 2-8 on the second floor. Under the system's influence, the smoke temperature dropped from the previous maximum of 30 °C to a maximum of 15 °C. The system effectively suppressed changes in the fire temperature and reduced the smoke temperature. Moreover, in terms of time, the system reached the temperature peak at around 300 s, while in the experiment without the system, the fire developed fully and reached its peak at around 400 s, a difference of approximately 100 s. However, the system failed to extinguish the fire in experiments 8-13

and 8-12 due to the high heat release rate. The temperature reached the standard for a second-level response at 200 s. The temperature difference before the second-level response was not significant at 2-2.7, but a noticeable change occurred after the second-level response started. Under the system's influence, the temperature at 2-7.5 was lower and less likely to cause combustibles to ignite. Thus, it can be concluded that the second-level response hindered the spread of the fire. This trend was also observed at other locations on the fire floor to varying degrees and was influenced by the system's water spray.

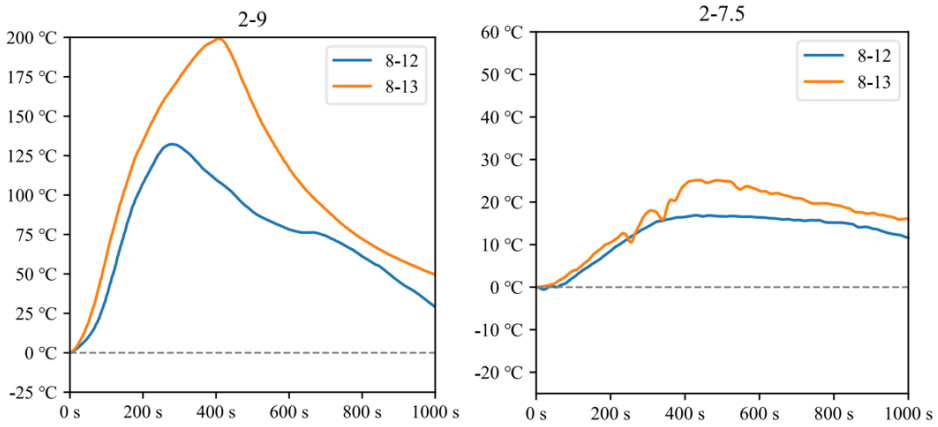

Figure 13. Temperature curves of rooms and corridors with ignition over time under experimental conditions 8-12 and 8-13.

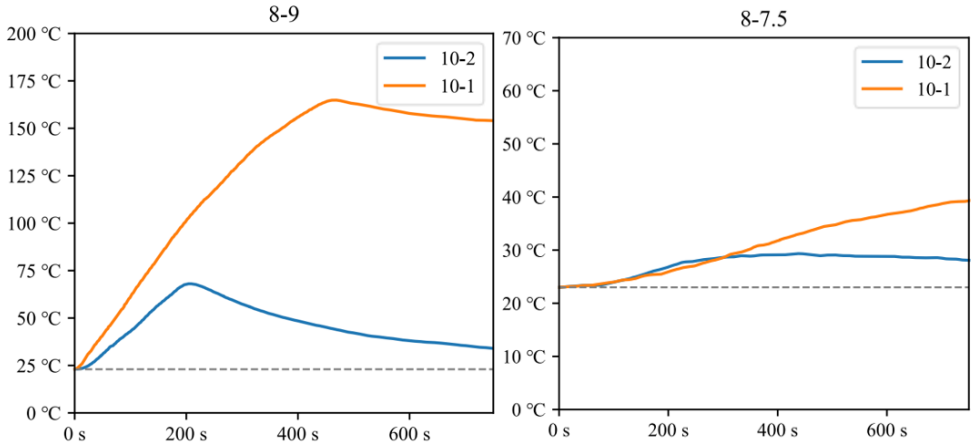

Figure 14. Temperature curves of rooms and corridors with ignition over time under experimental conditions 10-1 and 10-2.

Next, the case of a low heat release rate was considered. In Figure 14, it can be seen that room number 9 on the eighth floor was the fire room. Before the system was applied, the temperature in this room reached a maximum of 175 °C, but after the system was applied, the maximum temperature was only 70 °C. Similarly, the system effectively suppressed changes in the fire temperature, and a difference of 105 °C was observed in similar simulation experiments. It can be concluded that the system successfully extinguished the fire in experiments 10-1 and 10-2, where the heat release rate was low. In Figure 14, 8-7.5 represents the corridor between rooms 7 and 8 on the eighth floor. Under the system's influence, the smoke temperature dropped from the previous maximum of 40 °C to a maximum of 25 °C. However, the decrease in the corridor temperature in experiments 10-1 and 10-2 was not due to the second-level response of the system, but rather the result of the system extinguishing the fire. Moreover, in terms of time, the system reached the temperature peak at around 200 s, while in the experiment without the system, the fire developed fully and reached its peak at around 480 s, a difference of approximately 280 s.

This trend was also observed at other locations on the fire floor to varying degrees and was influenced by the system's water spray.

Based on the experimental results. It can be concluded that this system can effectively extinguish high-rise building fires. Even when fires develop rapidly and cannot be extinguished, the system's pre-response function can limit the fire to a certain area as much as possible. This provides valuable time for personnel evacuation from the high-rise building and external rescue efforts.

3.2.2. Impact of the System on Fire Smoke in High-Rise Buildings

Smoke particle concentration and visibility are two important physical parameters of smoke in addition to temperature [35]. This study analyzed the impact of the system on smoke particle concentration and visibility in high-rise building fires to explore whether the system could improve escape conditions for personnel during fires, reduce the danger of escape routes, and facilitate effective evacuation and rescue measures.

The smoke situation in the stairwell on the fire floor was analyzed. Particle concentration information was collected using the PMS7003T sensor, and the unit used was $\mu g/m^3$, which is the PM concentration. Table 5 shows the experimental conditions for comparing the 8-12 and 8-13 groups. The data were extracted according to the data frame description, and then filtered, and denoised, and the curves of each parameter during the experiment were plotted, as shown in Figure 15. In the preliminary stage of the simulation experiment, it was observed that the system had little effect on particles of different sizes, with only slight differences. However, in the later stage of the fire, at around 300 s, the system showed an accelerating settling trend for all particles. After 300 s, the system rapidly settled the curve, while the control group settled slowly. Additionally, the effect was more pronounced with higher particle concentration.

Table 5. Similar simulated experimental conditions for experiments 8-7 and 8-8.

Experiment Number	Fire Location	Heat Release Rate (kw)	System Response Status
8-12	(5.5)	5.7	Yes
8-13	(5.5)	5.7	No

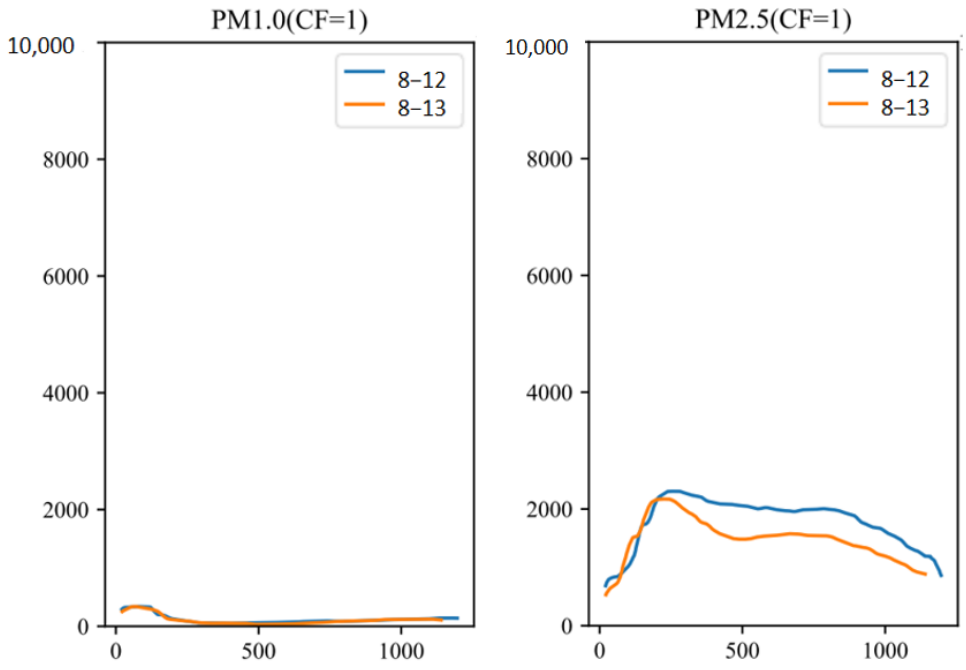

Figure 15. Comparison of particle concentration, at the vertical channel outlet between experiments 8-12 and 8-13.

The smoke visibility was measured in the experiment by measuring the illuminance of a constant light source passing through the smoke at a certain distance. The value measured by the OPT101 sensor in the experiment with a light path of 1 m was a simulated value. The smoke visibility was measured as a percentage, with 100% representing a lossless constant light source and 0% representing a completely dark environment. Table 6 shows the experimental conditions for experiments 9-8 and 9-10, and Figure 16 shows the comparison of the illuminance curves for these experiments. Figure 17 shows the situation of a constant light source in smoke.

Table 6. Similar simulated experimental conditions for experiments 9-8 and 9-10.

Experiment Number	Fire Location	Heat Release Rate (kw)	System Response Status
9-8	(8.5)	5.7	Yes
10-10	(8.5)	5.7	No

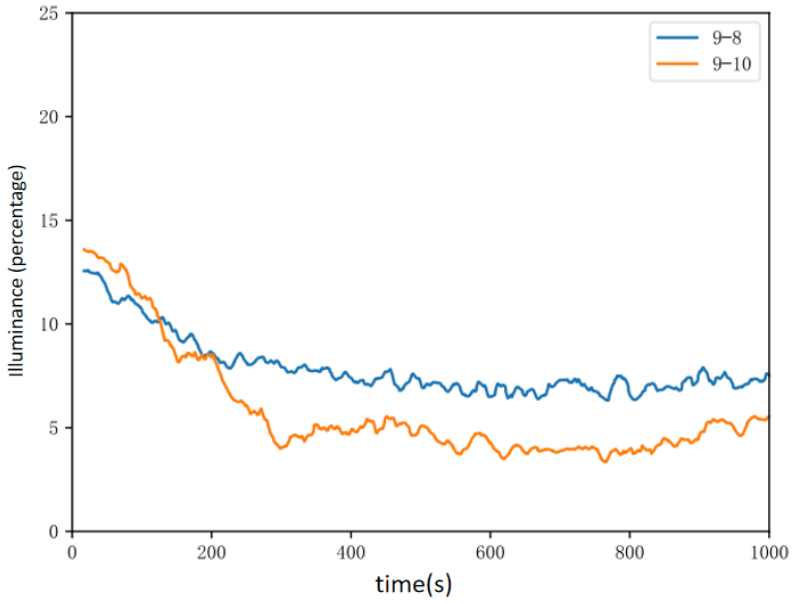

Figure 16. Comparison of illuminance change curves between experiments 9-8 and 9-10.

In summary of these four experiments, the impact of the system on smoke transport was obtained. From Section 3.2.1, it can be concluded that when the fire had a high heat release rate of 5.7 kW, the fire developed rapidly and the system could not quickly extinguish the fire. As time passed, the system reached a second-level response. Experiments 8-12, 8-13, 9-8, and 10-10, which had a heat release rate of 5.7 kW, activated the second-level response of the system. Under the second-level response, compared to the situation without the system, the particle concentration in the smoke decreased significantly, and the visibility increased significantly. Therefore, it can be concluded that the system obstructed the transmission of smoke. Slowing down the spread of smoke not only creates better conditions for personnel evacuation but also provides convenience for subsequent rescue work.

3.2.3. Response Time Analysis

This system is a real-time dynamic system, and its performance is directly affected by the response time. The time for a request and response is influenced by several factors, including network latency, the server response speed, the size and complexity of the request and response messages, and the performance of the browser [36]. Different requests and responses may have varying times. The time from information collection to action execution and disconnection needs to be within 1600 ms, which includes the 750 ms buffer waiting time set by the device. Therefore, the entire process takes approximately 2350 ms. Generally,

the system can respond rapidly within 3000 ms. By analyzing the statistical data of the received data time and response time from the first-level pre-response events extracted from all of the log data, Table 7 was obtained.

Figure 17. The situation of a constant light source in smoke.

Table 7. First-level pre-response time statistics for high-rise building fire simulation experiments.

Experiment Number	Accepted Data Time	Response Time	Time Difference (s)
7-11	16:13:09	16:13:12	3
7-11	16:14:09	16:14:11	2
7-11	16:15:54	16:15:56	2
7-13	16:56:37	16:56:40	3
8-2	11:22:12	11:22:15	3
8-2	11:26:25	11:26:26	1
8-5	12:34:51	12:34:52	1
8-5	12:36:53	12:36:54	1
8-5	12:40:46	12:40:47	1
8-7	13:44:37	13:44:40	3
8-7	13:47:28	13:47:30	2
8-9	14:38:24	14:38:26	2
8-9	14:44:25	14:44:26	1
8-9	14:46:27	14:46:28	1
8-9	14:53:07	14:53:08	1
8-9	14:57:25	14:57:26	1

Table 7. *Cont.*

Experiment Number	Accepted Data Time	Response Time	Time Difference (s)
8-10	15:56:19	15:56:20	1
8-10	16:03:33	16:03:34	1
8-12	16:54:58	16:55:01	3
8-14	17:56:23	17:56:24	1
8-14	17:58:39	17:58:42	3
8-14	18:06:22	18:06:25	3
9-4	15:44:02	15:44:04	2
9-4	15:49:58	15:50:01	3
9-6	16:35:26	16:35:28	2
9-6	16:40:16	16:40:19	3
9-8	17:34:10	17:34:12	2
9-11	18:46:41	18:46:42	1
9-11	18:51:04	18:51:05	1
10-2	9:37:46	9:37:47	1

The average response time of the system was calculated to be 2.0 s by analyzing the time difference in the response logs of the statistical system. This response speed is sufficiently agile when combined with pre-response strategies, making it suitable for dealing with complex high-rise building fires. Therefore, it can be concluded that this system has a sensitive response speed. As shown in Figure 16, there was no significant difference between the experimental and the control groups in the first 200 s after the system was started. The illuminance received by the OPT sensor in both groups fluctuated within a certain range. However, the experimental group showed a difference of approximately 3% in illuminance compared to the control group, indicating that fine water mist can reduce the shading effect of smoke to some extent in high-rise building fires.

4. Other System Functions

In addition to the basic functions of extinguishing fires and limiting the transmission of fires and smoke, this system has additional features. First, it has an independent power supply and communication system. All sensors and controllers of the system are connected to the ESP8266 chip. The chip's power supply and communication functions can be implemented using the same set of wires, without relying on the building's power supply equipment. As long as the fire control room uses an independent power supply, the system can have an independent power supply. Second, the system has dual power supply capabilities. Each chip is also connected to a battery as a backup power supply, which increases the system's reliability. Furthermore, the system has dual-channel communication capabilities. In addition to serial port communication between the ESP8266 and the control room, the system can also use Wi-Fi for wireless communication. By setting up an independent local area network outside the building, even if the communication lines are damaged or the fire control equipment is powered off, the wireless transmission can directly transmit the signal to the server. The simultaneous use of these two communication methods also increases the system's reliability. The system also has a data remote visualization function. Figure 18 is a screenshot of the MariaDB database used by the system. The database is established on a cloud server and can be accessed from anywhere with internet access using an IP address and a password. All data detected by the detectors and the actions of the actuators are stored in the database and updated in real time. During and after a fire, the database can be used to view the temperature and smoke conditions at different locations and times, which, to some extent, solves the problem of unclear fire conditions in fire rescue work. It is also helpful for post-fire investigation work.

log [@localhost] data [@localhost] × node [@localhost] console [@localhost]

1-500 of 501+ Tx: Auto DDL CSV

WHERE ORDER BY id DESC

	id 1	value	unit	sensor	time	raw	verify
1	2476224	25	Celsius	f2r10-thermocouple-2	2023-01-10 10:07:07	25	Lf2r10T4125
2	2476223	0	pa	gas-pressure-1	2023-01-10 10:07:06	0	LgasT4600
3	2476222	20.5	Celsius	f2r8-thermocouple-1	2023-01-10 10:07:06	20.5	Lf2r8T4203
4	2476221	9.75	Celsius	f9r9-thermocouple-1	2023-01-10 10:07:06	9.75	Lf9r9T4165
5	2476220	22	Celsius	f2r5-thermocouple-1	2023-01-10 10:07:06	22	Lf2r5T4174
6	2476219	21.75	Celsius	f2r6-thermocouple-1	2023-01-10 10:07:06	21.75	Lf2r6T3943
7	2476218	68.25	Celsius	f3r9-thermocouple-1	2023-01-10 10:07:06	68.25	Lf3r9T4137
8	2476217	22	Celsius	f2r4-thermocouple-1	2023-01-10 10:07:06	22	Lf2r4T4105
9	2476216	633	ug/m3	gas-PMS7003-2	2023-01-10 10:07:06	424d001…	gas4638617gas-…
10	2476215	13	Celsius	f9r3-thermocouple-1	2023-01-10 10:07:06	13	Lf9r3T4217
11	2476214	24.75	Celsius	f3r5-thermocouple-1	2023-01-10 10:07:06	24.75	Lf3r5T4164
12	2476213	12.5	Celsius	f9r7-thermocouple-1	2023-01-10 10:07:06	12.5	Lf9r7T4132
13	2476212	35.75	Celsius	f2r9-thermocouple-1	2023-01-10 10:07:06	35.75	Lf2r9T4147
14	2476211	12.5	Celsius	f9r1-thermocouple-1	2023-01-10 10:07:06	12.5	Lf9r1T4204
15	2476210	31	Celsius	f3r7-thermocouple-1	2023-01-10 10:07:06	31	Lf3r7T4195
16	2476209	11.25	Celsius	f9r5-thermocouple-1	2023-01-10 10:07:06	11.25	Lf9r5T4215
17	2476208	23	Celsius	f2r3-thermocouple-1	2023-01-10 10:07:06	23	Lf2r3T4173

Figure 18. Screenshot of MariaDB database.

5. Discussion

5.1. Innovation Points

This system introduces certain innovations in comparison to traditional high-rise building fire prevention and control systems. These innovations are mainly reflected in two aspects. First, a fire strategy for high-rise buildings was proposed and a system that combines fine water mist was designed. The system has real-time, dynamic, and pre-response characteristics and can implement different response strategies through built-in algorithms. Real-time data storage provides accurate and comprehensive data required for fire research, and the client provides a user-friendly human–computer interaction interface. The response strategy embodies the concept of hierarchical response. Second, the proposed pre-response strategy and designed system were tested and verified in a similar model of a high-rise building, and a simulation experiment verification system was designed. The experimental results demonstrate that the system performed as expected, providing useful guidance and experience for practical applications. Table 8 shows a comparison between this system and traditional fire control systems.

5.2. Precautions

Several key requirements need to be carefully considered in this system. First, due to the use of water mist nozzles, the system has a high water pressure requirement [37]. High water pressure is necessary for the formation of mist. Once there is a leak in the spray system pipeline, the hydraulic pressure will drop sharply, causing a significant loss of water flow. This can lead to a drastic decrease in system performance and even complete failure [38]. In practical applications, this type of accident can be fatal because once it occurs, the system cannot effectively suppress the fire. Second, the system has high water quality requirements. During the verification experiment, clogging of the fine water mist nozzles occurred due to impurities in the water, which blocked the filter element inside the nozzle. Therefore, it is necessary to strictly control the water quality of the water source in practical applications. Water containing a large amount of impurities should be filtered and purified before connecting it to the pipeline system to prevent nozzle blockage. Lastly, the system has high network requirements. As this system is based on the Internet of Things (IoT), it relies on the network for data transmission and storage through communication based on the HTTP protocol. The network can be a local area network (LAN), but a typical router can only support network connections for 30 or fewer devices. The solution is to replace the router and use mesh networking or deploy the server in a wide area network (WAN), allowing each device to work independently without interference. However, these methods will increase costs and installation complexity.

Table 8. Comparison between this system and traditional fire control systems.

Functional Characteristics	Traditional Fire Control System	Real-Time Pre-Response System for High-Rise Building Fires Based on the Internet of Things
Initiative	Traditional fire control systems achieve passive activation by installing temperature-sensitive glass tubes or metal on the nozzle, lacking initiative.	In the event of a fire, areas that are not directly affected by the fire can be actively controlled by studying the fire path to prevent the spread of smoke and fire.
Visuality	Fires often generate a large amount of smoke, which, in severe cases, damages the power system and decreases visibility.	Due to the ability of physical devices to collect environmental information through the internet and upload it to the server, the system can penetrate the shielding of building walls and timely detect fire information.
Dynamicity	The spray system switch in traditional fire control systems is disposable and will not automatically close after it has started.	The control system can dynamically follow the fire situation, and when the fire is extinguished, the fire control device can be turned off in a timely manner to save water and water pressure.
Reproducibility	Buildings equipped with traditional fire control systems can only determine the fire situation through the traces of combustion after experiencing a fire.	The integrated system can store the environmental information during a fire and restore the fire scene through modeling after the fire ends, thereby analyzing the cause of the accident and preventing future fires.

5.3. Further Research and Development Scope

Currently, the system is equipped only with fine water mist devices as actuators. However, additional actuators can be incorporated into the system. Collected signals can be used to dynamically adjust other devices, such as mechanical ventilation and smoke exhaust systems, and evacuation indicators, through built-in server algorithms. By connecting other devices to the system, it can more effectively extinguish fires or confine them to a certain area, providing better conditions for personnel evacuation and firefighting rescue work. This system is currently in the experimental stage and has only been used on a similar simulation platform we built ourselves. It has not yet been implemented in actual buildings. Once improved and tested, it will be used as a product in construction.

6. Conclusions

This paper presents the development of a real-time dynamic pre-response system for high-rise buildings based on the Internet of Things. The system can quickly detect and predict fires, and pre-spray fine water mist along the path of fire and smoke transmission to prevent their spread. We also designed experiments to verify the system's ability to extinguish fires and prevent fire and smoke propagation. The main conclusions are as follows:

(1) Compared to conventional fire control systems, the system's greatest advantage lies in its ability to dynamically adjust the fine water mist nozzles in real time and initiate action based on the built-in algorithm. This approach can limit fires and smoke to a certain area, even in cases where the fire develops rapidly and cannot be extinguished quickly. Moreover, the system's real-time dynamic adjustment capability can prevent fire re-ignition.

(2) Based on the results obtained from a similar simulation experimental platform, the system could extinguish ordinary fires. In cases where the fire was larger, the system could prevent or slow down the spread of fire and smoke to other rooms and floors, providing valuable time for personnel evacuation and rescue work.

(3) The system's independent power supply, dual power supply, and dual-channel communication functions increase the overall stability and reliability of the system. Furthermore, some of the system's functions improve the problem of unclear fire situations during high-rise fires to some extent, providing important reference information for rescue work and fire extinguishing, and further ensuring rescue safety.

Author Contributions: J.Z. wrote the program and conceived the methodology; H.Z. conceptualized the methodology, conducted the experimental simulations and data processing, wrote the paper; supervision, Z.Y. All authors have read and agreed to the published version of the manuscript.

Funding: This research was funded by the Guizhou Province Science and Technology Support Project (Qiankehe Support (2021) 519).

Institutional Review Board Statement: Not applicable.

Informed Consent Statement: Not applicable.

Data Availability Statement: Not applicable.

Conflicts of Interest: The authors declare no conflict of interest.

References

1. Jonsson, A.; Runefors, M.; Gustavsson, J.; Nilson, F. Residential fire fatality typologies in Sweden: Results after 20 years of high-quality data. *J. Saf. Res.* **2022**, *82*, 68–84. [CrossRef]
2. Templeton, A.; Nash, C.; Lewis, L.; Gwynne, S.; Spearpoint, M. Information sharing and support among residents in response to fire incidents in high-rise residential buildings. *Int. J. Disast Risk Reduct.* **2023**, *92*, 103713. [CrossRef]
3. Templeton, A.; Nash, C.; Spearpoint, M.; Gwynne, S.; Hui, X.; Arnott, M. Who and what is trusted in fire incidents? The role of trust in guidance and guidance creators in resident response to fire incidents in high-rise residential buildings. *Saf. Sci.* **2023**, *164*, 106172. [CrossRef]
4. Zhao, H.; Tong, J.; Zhao, J.; Wu, J. Failure characteristic of class 1E electrical cable used in the nuclear power plant exposed to fire. *Prog. Nucl. Energ.* **2022**, *150*, 104292. [CrossRef]
5. Alianto, B.; Nasruddin, N.; Nugroho, Y.S. High-rise building fire safety using mechanical ventilation and stairwell pressurization: A review. *J. Build. Eng.* **2022**, *50*, 104224. [CrossRef]
6. Sun, X.; Cai, N.; Zhang, W. Discussing the development of domestic and foreign fire protection technical regulation and fire protection technical standard systems. *J. Saf. Sci. Resil.* **2023**, *4*, 26–29. [CrossRef]
7. Arewa, A.O.; Ahmed, A.; Edwards, D.J.; Nwankwo, C. Fire Safety in High-Rise Buildings: Is the Stay-Put Tactic a Misjudgement or Magnificent Strategy? *Buildings* **2021**, *11*, 339. [CrossRef]
8. Liu, X.; Xu, Z.; Sun, B.; Liu, X.; Xu, D. Smart prediction for tunnel fire state evolution based on an improved fire simulation curve through particle swarm optimization algorithm. *Fire Saf. J.* **2023**, *136*, 103763. [CrossRef]
9. Hassan, M.K.; Hossain, M.D.; Gilvonio, M.; Rahnamayiezekavat, P.; Douglas, G.; Pathirana, S.; Saha, S. Numerical Investigations on the Influencing Factors of Rapid Fire Spread of Flammable Cladding in a High-Rise Building. *Fire* **2022**, *5*, 149. [CrossRef]
10. Wegrzynski, W.; Antosiewicz, P.; Burdzy, T.; Tofilo, P.; Papis, B.K. Experimental investigation into fire behaviour of glazed facades with pendant type sprinklers. *Fire Saf. J.* **2020**, *115*, 103159. [CrossRef]
11. Hsiao, C.; Hsieh, S. Real-time fire protection system architecture for building safety. *J. Build. Eng.* **2023**, *67*, 105913. [CrossRef]
12. Forrest, B.; Weckman, E.; DiDomizio, M.; Senez, P.; Ryder, N. Smoke development and movement during ventilation-limited fires in a multi-storey house. *Fire Mater.* **2021**, *45*, 1063–1074. [CrossRef]
13. Jiang, L.; Shi, J.; Wang, C.; Pan, Z. Intelligent control of building fire protection system using digital twins and semantic web technologies. *Autom. Constr.* **2023**, *147*, 104728. [CrossRef]
14. Kuznetsov, G.; Kopylov, N.; Sushkina, E.; Zhdanova, A. Adaptation of Fire-Fighting Systems to Localization of Fires in the Premises: Review. *Energies* **2022**, *15*, 522. [CrossRef]
15. Zheng, D.; Yan, W. Intelligent Monitoring System for Home Based on FRBF Neural Network. *Int. J. Smart Home* **2015**, *9*, 207–218. [CrossRef]
16. Khan, A.A.; Khan, M.A.; Leung, K.; Huang, X.; Luo, M.; Usmani, A. A review of critical fire event library for buildings and safety framework for smart firefighting. *Int. J. Disast Risk Reduct.* **2022**, *83*, 103412. [CrossRef]
17. Zhou, F.; Li, J.; He, S.; Liu, Y. Experimental modeling study on the reignition phenomenon when opening a sealed fire zone. *Procedia Earth Planet. Sci.* **2009**, *1*, 161–168. [CrossRef]
18. Espejo, V.; Vilchez, J.A.; Casal, J.; Planas, E. Fired equipment combustion chamber accidents: A historical survey. *J. Loss Prev. Proc.* **2021**, *71*, 104445. [CrossRef]
19. Zhu, J.; Song, Y.; Wang, J.; Yang, Q.; Ma, S.; Zhang, S.; Chen, T.; Jia, Z. A highly flame-retardant, agile fire-alarming and ultrasensitive cotton fabric-based piezoresistive sensor for intelligent fire system. *Polym. Degrad. Stabil.* **2023**, *211*, 110338. [CrossRef]
20. Servida, F.; Fischer, M.; Delémont, O.; Souvignet, T.R. Ok Google, Start a Fire. IoT devices as witnesses and actors in fire investigations. *Forensic Sci. Int.* **2023**, *348*, 111674. [CrossRef]
21. Perassi, A.; Cacciabue, P.C. Cognitive Ergonomics Principles for Re-Designing Function Allocation and Interfaces of a Fire Fighting Control Room of a Large City. *IFAC Proc. Vol.* **2001**, *34*, 429–434. [CrossRef]

22. Pereira, D.M.; Vieira, M.B.; Villela, S.M. Combining Neural Networks and a Color Classifier for Fire Detection. In *Intelligent Systems, PT II, Proceedings of the 11th Brazilian Conference on Intelligent Systems (BRACIS), Campinas, Brazil, 28 November–1 December 2022*; Xavier-Junior, J.C., Rios, R.A., Eds.; Springer: Cham, Switzerland, 2022; Volume 13654, pp. 139–153. [CrossRef]
23. Shaharuddin, S.; Abdul Maulud, K.N.; Syed Abdul Rahman, S.A.F.; Che Ani, A.I.; Pradhan, B. The role of IoT sensor in smart building context for indoor fire hazard scenario: A systematic review of interdisciplinary articles. *Internet Things* **2023**, *22*, 100803. [CrossRef]
24. West; Brent, D. *Introduction to Graph Theory*; Longman: New York, NY, USA, 1985.
25. Hosouli, S.; Elvins, J.; Searle, J.; Boudjabeur, S.; Bowyer, J.; Jewell, E. A Multi-Criteria decision making (MCDM) methodology for high temperature thermochemical storage material selection using graph theory and matrix approach. *Mater. Des.* **2023**, *227*, 111685. [CrossRef]
26. Bonato, A.; Messinger, M.; Prałat, P. Fighting constrained fires in graphs. *Theor. Comput. Sci.* **2012**, *434*, 11–22. [CrossRef]
27. Mcgrattan, K.B. *Fire Dynamics Simulator (Version 4)—Technical Reference Guide*; Nist Special Publication; National Institute of Standards and Technology: Gaithersburg, MD, USA, 2005.
28. Asensio, M.I.; Cascón, J.M.; Laiz, P.; Prieto-Herráez, D. Validating the effect of fuel moisture content by a multivalued operator in a simplified physical fire spread model. *Environ. Modell. Softw.* **2023**, *164*, 105710. [CrossRef]
29. Zhang, Y.; Zhang, X.; Wang, L. Experimental validation and simplified design of an energy-based time equivalent method applied to evaluate the fire resistance of the glulam exposed to parametric fire. *Eng. Struct.* **2022**, *272*, 115051. [CrossRef]
30. Shields, T.J. Victims and survivors in fatal residential building fires. *Fire Mater.* **1999**, *23*, 305–310.
31. Xiang, M.; Zhang, B.; Guo, X. Infinitely many solutions for a fractional Kirchhoff type problem via Fountain Theorem. *Nonlinear Anal. Theory Methods Appl.* **2015**, *120*, 299–313. [CrossRef]
32. Sastri, Y.; Kuttyamma, A.J. NetworkX and Matplotlib an Analysis. *Int. J. Sci. Eng. Res.* **2013**, *4*.
33. Lin, P.; Xiong, Y.; Zuo, C.; Shi, J. Verification of Similarity of Scaling Laws in Tunnel Fires with Natural Ventilation. *Fire Technol.* **2021**, *57*, 1611–1635. [CrossRef]
34. Li, Q.; Kang, J.; Wang, Y.; Feng, Y. Superheated steam similarity simulation on longitudinal distribution of maximum smoke temperature rise in tunnel fires. *Therm. Sci. Eng. Prog.* **2023**, *37*, 101550. [CrossRef]
35. Ji, J.; Lu, W.; Li, F.; Cui, X. Experimental and numerical simulation on smoke control effect and key parameters of Push-pull air curtain in tunnel fire. *Tunn. Undergr. Sp. Tech.* **2022**, *121*, 104323. [CrossRef]
36. Veeramanikandan; Sankaranarayanan, S.; Rodrigues, J.J.P.C.; Sugumaran, V.; Kozlov, S. Data Flow and Distributed Deep Neural Network based low latency IoT-Edge computation model for big data environment. *Eng. Appl. Artif. Intel.* **2020**, *94*, 103785. [CrossRef]
37. Alenezi, M.H.; Sadek, H. Fire-suppression performance of high-pressure water mist system inside scaled-down road tunnel section. *J. Eng. Res.-Kuwait* **2023**, *11*, 100024. [CrossRef]
38. Huo, Y.; Chen, M.; Li, T.; Zou, G.; Dong, H. Experimental study on fire suppression performance of the high pressure water mist in the engine room of an offshore platform. *J. Loss Prevent Proc.* **2023**, *83*, 105052. [CrossRef]